

Cation adsorption on oxides and clays: The aluminum case

L. Charlet¹, P. W. Schindler, L. Spadini¹, G. Furrer² and M. Zysset³

Institut of Inorganic, Analytical and Physical Chemistry, University of Bern, CH-3000 Bern 9, Switzerland

¹ Environmental Geochemistry Group, LGIT, University of Grenoble (UJF), F-38041 Grenoble, France

² Institute of Terrestrial Ecology, ETH Zürich, Grabenstr. 3, CH-8952 Schlieren, Switzerland

³ Federal Institute for Forestry Research, WSL, Zürcherstrasse 111, CH-8903 Birmensdorf, Switzerland

Key words: Surface complexation, montmorillonite, silica, aluminum, proton surface charge.

ABSTRACT

The sorption mechanisms for trace metal ions on montmorillonite have been investigated. Complexation with surface hydroxyl groups located on the broken edges of platelet particles is found to occur over a pH range similar to that observed on silica and other oxides, at comparable metal/site ratios. A second mechanism involving cation exchange on the negatively charge basal plane, which does not involve proton exchange in our experimental conditions, has been invoked to explain the low pH behavior. Consistent with this cation exchange mechanism, adsorption at low pH is strongly ionic strength dependant. A quantitative model which involves both mechanisms is presented and tested against both cation and proton adsorption data.

Introduction

Because of their importance for industry and natural systems, a great deal of effort has been devoted characterizing the surface chemistry of oxides and clays. The adsorptive properties of clays such as montmorillonite are, to a large extent, dominated by their permanent structural negative charge arising from isomorphic substitution within the lattice. Except for alkali metals, cations sorbed onto the basal plane of montmorillonite do not lose, in water saturated systems, the water molecules of their inner hydration shell (Sposito, 1984). They are sorbed via an outer-sphere complex structure that has been investigated by neutron scattering, ESR and EXAFS (Sposito, 1984; McBride, 1991; Dent et al., 1992). On the other hand, the surface charge of oxides, and presumably of clay crystal broken edges, results from protonation/deprotonation of surface hydroxyl groups. Hydrated cations sorbed onto oxide surfaces have been to date found to form inner-sphere surface complexes

(Motschi, 1987; Charlet and Manceau, 1993). The difference between outer- and inner-sphere surface complexation has profound implications on the modeling of the chemical properties of natural fluids and mineral assemblages. To facilitate computer prediction of sorption reactions, the classical thermodynamic treatment of cation exchange on clay has been combined with the surface complexation models (Shaviv and Mattigod, 1985; Schindler et al., 1987; Fletcher and Sposito, 1989). This combined model has been previously tested against data pertaining to cation depletion in solution (Fletcher and Sposito, 1989) but not, to our knowledge, against data related to the proton release that occurs upon cation adsorption.

Among cations, aluminum plays a key role in geochemistry, because of its abundance and of the toxicity of the free Al^{3+} ion to various living organisms. Dissolved aluminum in the ocean is presumably scavenged by biogenic silica particles. When adsorbed onto silica, aluminum may inhibit the crystal growth (Brown and Thomas, 1960) or the dissolution of silica particles (Iler, 1973) depending on whether the solution is undersaturated or oversaturated with respect to the silica phase. The inhibition of K-montmorillonite dissolution by Al(III) has also been observed (Zysset, 1992; Furrer, this volume).

In this paper we report adsorption data from aluminum ions and protons on montmorillonite and on silica under conditions where (i) polymerization does not yet occur and (2) saturation of the surface hydroxyl sites has not been reached. These conditions are particularly true for experiments with montmorillonite which were done in conditions undersaturated with respect not only to total surface sites, but also to total surface edge sites. Our objectives are (i) to quantify surface-induced hydrolysis in terms of surface complexation constants, and (ii) to compare Al adsorption on montmorillonite and silica particles, and thus to give new insights into the chemistry of clay edges.

Experimental

Amorphous silica ("Aerosil 400") was supplied by Degussa Co. (Frankfurt). The BET specific surface given by the producer was: $s = 400 \text{ m}^2 \text{ g}^{-1}$. Silica was freeze dried after suspension in double deionized water to allow reproducible sampling.

Bentonite (Wyoming montmorillonite, SWy-1) was provided by the Clay Mineral Society (USA). Molar chloride suspensions of the $< 2 \mu\text{m}$ fraction of the K^+ -saturated montmorillonite was prepared according to Sposito (1981). The concentration was then lowered to the desired value by about five equilibrations with 0.03 M KCl or 0.1 M KCl[†]. The clay was stored as clay suspensions. The measured cation exchange capacity of the clay was: $0.952 \pm 0.009 \text{ eq/g}$ (Zysset, 1992).

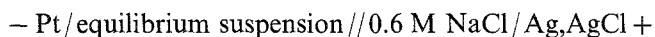
The stock solution of AlCl_3 was prepared from $\text{AlCl}_3 \cdot 6\text{H}_2\text{O}$ (p.a. Merck) and acidified with a known amount of acid. The Al(III) concentration was determined by an ion exchange method, passing a known aliquot through a column containing Dowex 50 W (Fluka). Solutions of HCl and NaOH were prepared from Titrisol

[†] Details on the method can be obtained from the senior author

(Merck). All solutions were prepared using bidistilled water. NaCl (silica experiments) or KCl (montmorillonite experiments) were added to the particle suspensions to minimize variations in the activity coefficients of solution species and to maintain a sufficient electric conductivity.

The potentiometric titrations were performed with an automated system consisting of an IBM XT compatible PC, a Keithley Scanner Model 705, 224 programmable current source and System 196 digital multimeter. The titration cell was kept at 25.0 ± 0.1 °C. The concentration of hydrogen ions was measured using a Metrohm type T glass electrode combined with an amplifier (AD515 KH). For each titration, the standard potential E° of the glass electrode was evaluated by the Gran method between pH 2.7 and 3.0 either in the background solution or directly in the experimental suspension (silica experiments).

Potentiometric titrations were carried out on suspensions which were made by addition of NaCl or KCl solutions and HCl/AlCl₃ stock solution to dry silica or aliquots of montmorillonite suspension. The general composition of these suspensions is given by the solid concentration a (g dm⁻³), the total aluminum concentration Al_t (M), the total chloride concentration Cl_t (M), the initial proton concentration H₀ (M), given by the amount of added HCl, and the total concentration of Na⁺ (M) and K⁺ (M), respectively, given by the ion balance ($= \text{Cl}_t - \text{H}_0 - 3 \cdot \text{Al}_t$). After one hour equilibration time the total proton concentration was partially neutralized ($\text{H}_t = \text{H}_0 - [\text{OH}^-]_c$) by coulometrically generated hydroxide ions ($[\text{OH}^-]_c$) with the cell



where the double forward slash indicates a liquid junction (salt bridge). In order to prevent a local excess of base that might result in the precipitation of Al(OH)₃(s), the current was limited to 2.5 mA and the titrations stirred with a suspended Teflon propeller. Argon gas after passing through a solution with an ionic strength similar to the reacting suspension was used to maintain an inert atmosphere. The hydrogen ion concentration $[\text{H}^+]$ (M) was measured with the aid of a combined glass electrode. In this paper, pH is used to refer to $-\log [\text{H}^+]$, i.e. to a concentration scale. Equilibrium was assumed when the electrode potential drifted less than 1 mV/h. It could take as much as 6 h in the case of silica experiments. If K_w denotes the ionic product of water valid for the ionic strength used in the experiment, then H_s , the net concentration of protons released from the surface in mol/l is defined by

$$\text{H}_s = [\text{H}^+] - \text{H}_t - K_w [\text{H}^+]^{-1} \quad (1)$$

Net proton adsorption data are presented in plots depicting H_s/a or $\text{H}_s/[\text{Al}]_t$ as a function of pH. Some titrations were performed in the discontinuous mode. After equilibration at the desired pH value an aliquot of the suspension was filtered (0.01 µm) and the total aluminum concentration was measured colorimetrically (Dougan and Wilson, 1974).

Data treatment

Amphoteric surface sites $\equiv \text{SOH}$. Terminal hydroxyl groups and terminal water molecules can be visualized as protruding out of silica and montmorillonite edge surfaces (Sposito, 1984, White and Zelazny, 1988). A moiety containing one or several groups is symbolized by $\equiv \text{SOH}$ (S = Si, Al). Equilibria between $\equiv \text{SOH}$, Al^{3+} and H^+ can be described by:

$$p \equiv \text{SOH} + q \text{Al}^{3+} + r \text{H}^+ = (\equiv \text{SOH})_p \text{Al}_q \text{H}_r^{(3q+r)+} \quad \beta_{pqr}^s \quad (2)$$

For statistical reasons, p needs to be always 1. Acid-base equilibria are defined by:

$$\equiv \text{SOH} + r \text{H}^+ = \equiv \text{SOH}_{r+1}^+ \quad \beta_{10r}^s \quad (3)$$

The total concentration of the components is given by:

$$[\equiv \text{SOH}]_t = \sum_p \sum_q \sum_r p \beta_{pqr}^s [\equiv \text{SOH}]^p [\text{Al}^{3+}]^q [\text{H}^+]^r \quad (4)$$

$$\text{Al}_t = \sum_p \sum_q \sum_r q \beta_{pqr}^s [\equiv \text{SOH}]^p [\text{Al}^{3+}]^q [\text{H}^+]^r \quad (5)$$

$$\text{H}_t = \sum_p \sum_q \sum_r r \beta_{pqr}^s [\equiv \text{SOH}]^p [\text{Al}^{3+}]^q [\text{H}^+]^r \quad (6)$$

The conditional constants in Equations (2) to (6) need to be corrected for the coulombic energy of the charged surface to obtain the corresponding intrinsic constants:

$$\beta_{pqr(\text{int})}^s = \beta_{pqr}^s e^{((3q+r)F\psi/RT)} \quad \text{for all species with } p \neq 0 \quad (7)$$

ψ is the acting surface potential. The surface charge is given (in the units of M) by:

$$T_\sigma = \sum_{p \neq 0} \sum_q \sum_r (3q+r) \beta_{pqr}^s [\equiv \text{SOH}]^p [\text{Al}^{3+}]^q [\text{H}^+]^r \quad (8)$$

or in units of C/m², by

$$\sigma = \frac{T_\sigma \cdot F}{s \cdot a} \quad (9)$$

where s is the specific surface area (m²/g) and F is the Faraday constant. As will be shown later, Al adsorbs at the silica and montmorillonite edge surfaces essentially between pH 3.5–5.0, where Al-free silica surface is approximately neutral and the crystal edge surface of montmorillonite is positively charged. This excludes the formation of outer-sphere complexes. The data were modeled using the constant

capacitance model (Schindler and Gamsjäger, 1972). Within this model charge and potential of the surface are related by:

$$\sigma = \kappa \cdot \psi \quad (10)$$

where κ (C m^{-2}) represents the capacitance. Combining Eqs. (9) and (10) yields:

$$\psi = \frac{T_\sigma \cdot F}{s \cdot a \cdot \kappa} \quad (11)$$

The intrinsic stability constants, the total concentration of sites $[\equiv \text{SOH}]_t$, and the capacitance κ were evaluated using the program GRFIT (Ludwig, pers. communication). The evaluation was based on the proton balance and goodness of fit (Westall, 1982).

Weak acid sites $\equiv XH$. On montmorillonite, speciation calculations were performed with two surface sites, $\equiv \text{SOH}$ and $\equiv XH$. The stoichiometric replacement of K^+ by Al^{3+} on montmorillonite basal planes is described by:



where $\equiv X^-$ is an hypothetical aqueous species representing one mole of structural surface charge with unit valency (Fletcher and Sposito, 1989) and properties of a weak acid (Schindler et al., 1987). The thermodynamic equilibrium constant for this reaction is:

$$K_a = \frac{(x_{\text{Al}} \cdot f_{\text{Al}}) \cdot ([\text{K}^+] \cdot \gamma_{\text{K}})^3}{(x_{\text{K}} \cdot f_{\text{K}})^3 \cdot ([\text{Al}^{3+}] \cdot \gamma_{\text{Al}})} \quad (13)$$

where x_{K} and x_{Al} are the mole fractions on the exchanger phase, f_{K} and f_{Al} the rational activity coefficients of the surface species and γ_{K} and γ_{Al} the single-ion activity coefficients. The Vanselow coefficient is the conditional equilibrium constant defined by:

$$K_v = \frac{[(\equiv X)_3 \text{Al}] \cdot ([\text{K}^+] \cdot (\gamma_{\text{K}}))^3}{[\equiv XK]^3 \cdot ([\text{Al}^{3+}] \cdot \gamma_{\text{Al}})} \cdot ([\equiv XK] + [(\equiv X)_3 \text{Al}])^2 \quad (14)$$

If $[\equiv XK] \gg [(\equiv X)_3 \text{Al}]$, Equation (14) reduces to:

$$K_v = \frac{[(\equiv X)_3 \text{Al}] \cdot ([\text{K}^+] \cdot (\gamma_{\text{K}}))^3}{[\equiv XK] \cdot ([\text{Al}^{3+}] \cdot \gamma_{\text{Al}})} \quad (15)$$

Solution chemistry. The (0,1,1), (0,1,2), (0,1,3) and (0,1,4) hydrolysis and (0,3,4) polymerization constants were taken as equal, in a 0.6 M NaCl ionic medium, to: 5.52, 10.64, 16.34, 23.89 and -13.57 respectively (Lövgren et al., 1991), and at 0 M equal to: 5.01, 10.10, 16.16, 22.15 (Wolery et al., 1992) and -13.8 (CHEMVAL, pers. communication). Single ion activity coefficients at 0.01 and 0.1 M were calculated

using the Davis equation. The 1 M activity coefficients were computed according to the specific interaction theory (Biederman et al., 1982). These corrected values compare well with the (0,1,1) and (0,3,4) obtained experimentally by Hedlund (1988) at 0.01, 0.1 and 1 M: 5.1 and -13.7 , 5.3 and -13.6 , and 5.5 and -13.6 , respectively.

Results

Adsorption of aluminum on silica. Titration curves of silica performed in presence of aluminum indicate the release of three protons per adsorbed Al, once all aluminum ions are adsorbed (Fig. 1a). In absence of aluminum, proton titrations of silica measured at three solid concentrations: 1, 15 and 50 g l^{-1} (data not shown) lead, according to the linear regression method (Schindler and Stumm, 1987), for the deprotonation constant to a $\log \beta_{10-1}^s$ (i.e., $\log K_{a2}^{\text{int}}$) value of -6.97 ± 0.09 for all solid concentrations, a value in good agreement with previously published values (see e.g. Schindler and Stumm, 1987). Each titration curve performed in presence of aluminum (Experiments 4 to 9 in Table 1) could be fitted individually, assuming two simultaneous sorption mechanisms for Al^{3+} , namely Equation (2) with $pqr = 1, 1, -2$ and $1, 1, -3$. The computed curves (Fig. 1b) were obtained with $\log \beta_{1,1,-3}^s$ values equal to -10.57 , -10.73 , -10.55 , -10.04 , -9.37 and -8.76 for Experiments 4 to 9, i.e. for aluminum maximum coverage equal to 56, 19, 7, 3 and 1 % of the surface sites, respectively (Table 1), assuming a double layer of 0.4 F m^{-2} specific capacitance. The increase in complexation stability constant with decrease in surface coverage may indicate the existence of „high energy surface sites”, i.e. sites characterized by a high $\beta_{1,1,-3}^s$ value. These complexation constants, obtained on the

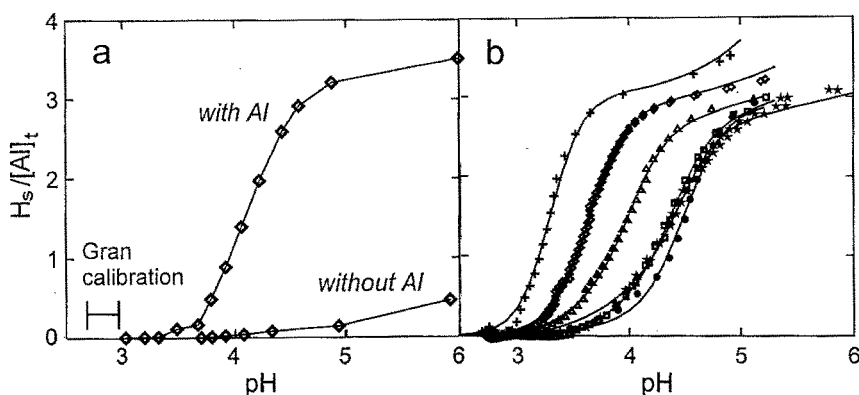


Figure 1. Proton surface charge on silica: (a) in absence or presence of aluminum; the H_s values in both cases are divided by the total aluminum concentration ($92.3 \mu\text{M}$) present in the later experiment. Solid concentration: 1 g/l. (b) Same titration curves but measured at different aluminum to silica ratio, i.e. at different total added aluminum concentration and different solid concentrations (from right to left, experiments No 4 to 9; Table 1). All experimental data (symbols) were measured in a 0.6 M NaCl background ionic medium. Lines are modeled curves (model: solution equilibria and Equations 2 and 3).

Table 1. Experimental conditions

Exp. No	Solid	<i>a</i> (g/l)	[Al] _t (μM)	Al _t [≡SOH] _t	[Cl ⁻] _t (M)	ionic medium
1	silica	1	0	0	0.6	NaCl
2	silica	15	0	0	0.6	NaCl
3	silica	50	0	0	0.6	NaCl
4	silica	1	837.5	0.56	0.6	NaCl
5	silica	1	230	0.15	0.6	NaCl
6	silica	1	112	0.076	0.6	NaCl
7	silica	1	57	0.076	0.6	NaCl
8	silica	15	750	0.033	0.6	NaCl
9	silica	50	837.5	0.011	0.6	NaCl
10	K-montmorillonite	1.95	0	0*	0.03	KCl
11	K-montmorillonite	1.95	11.2	0.066*	0.03	KCl
12	K-montmorillonite	1.95	30.7	0.18*	0.03	KCl
13	K-montmorillonite	1.95	105.5	0.63*	0.03	KCl
14	K-montmorillonite	2.03	0	0*	0.1	KCl
15	K-montmorillonite	2.03	15.8	0.09*	0.1	KCl
16	K-montmorillonite	2.03	32.5	0.19*	0.1	KCl
17	K-montmorillonite	2.03	105.6	0.60*	0.1	KCl
18	K-montmorillonite	1.86	0	0*	1	KCl
19	K-montmorillonite	1.86	16.0	0.10*	1	KCl
20	K-montmorillonite	1.86	41.36	0.26*	1	KCl
21	K-montmorillonite	1.86	113.2	0.70*	1	KCl
22 [‡]	lepidocrocite	10	440	0.47	0.6	NaCl
23 [¶]	goethite		320	0.40	0.6	NaCl

* On the basis of $(>\text{SOH})_t = 86.4 \mu\text{mol g}^{-1}$ for edges (see text).

[‡] Data from Zhang et al., 1992.

[¶] Data from Lövgren et al., 1990.

basis of proton balance data, adequately predict the aluminum adsorption data (Fig. 2, upper left). The step in the adsorption curves is shifted to the acid side as the solid concentration is increased and, to a smaller extent, as the total aluminum concentration is decreased (Fig. 1 b).

Adsorption of aluminum onto montmorillonite. Aluminum adsorption curve on montmorillonite were measured for various background ionic strengths, and at three total aluminum concentrations (10 to 110 μM; see Tab. 1). Little differences are observed among the three curves recorded at the same ionic strength, while a striking effect is observed for different ionic strengths (Fig. 3).

In molar KCl solutions, montmorillonite behaves very similar to silica or lepidocrocite, with respect to Al adsorption (Fig. 2, upper left corner and Fig. 3). The proton surface charge curves (Fig. 4a) are also very similar to those observed with goethite or lepidocrocite (Lövgren et al., 1991; Zhang et al., 1992). At pH less than 3.75 (no adsorption) or larger than 5.5 (99% Al adsorbed), the curves run parallel to the titration curve obtained in absence of dissolved Al. Within this pH range, titration curves diverge considerably. The adsorption of Al on montmorillonite and the consecutive proton release are adequately described by Equation (2) with

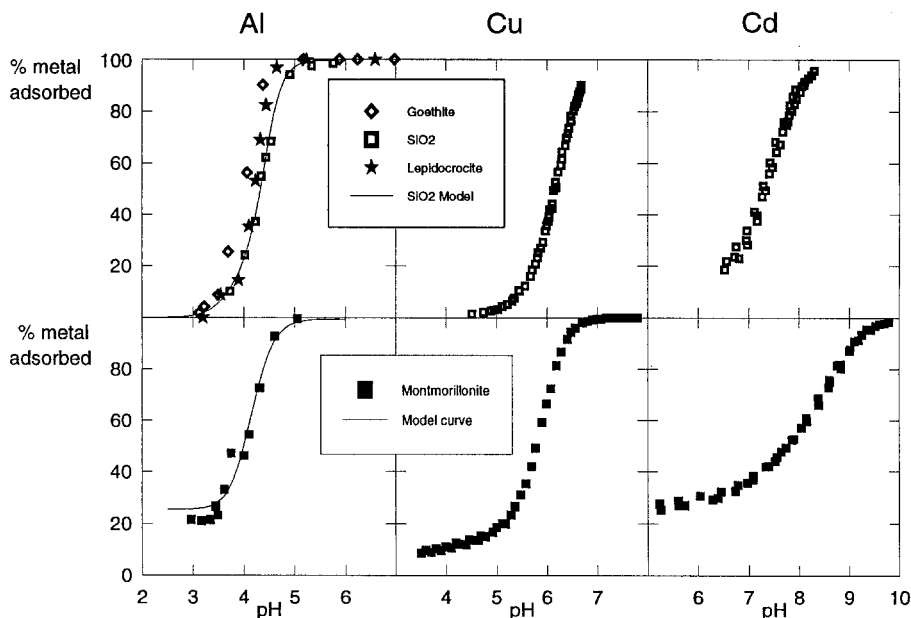


Figure 2. Adsorption of Al, Cu and Cd on montmorillonite (lower graphs) and various (oxyhydr)oxides (upper graphs). On montmorillonite the metal surface coverage is in these experiments always below the saturation of the edge sites, and adsorption is dominated (i) at low pH values by cation exchange on the basal plane, and (ii) at higher pH values by surface complexation on edges (data from Lövgren et al., 1991; Schindler et al., 1976; Stadler et al., 1993; Zhang et al., 1992; and this study).

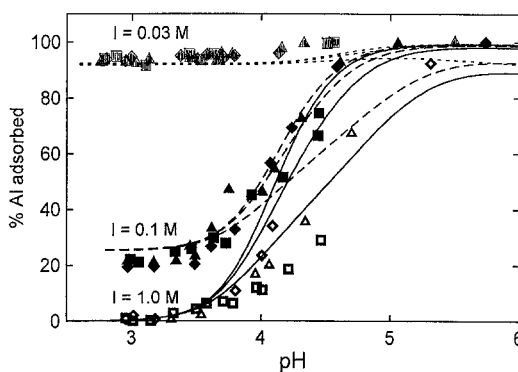


Figure 3. Adsorption of aluminum on montmorillonite at three different ionic strengths (0.03 mol l^{-1} KCl: empty symbols, top curves; 0.1 mol l^{-1} KCl: full symbols; 1 mol l^{-1} KCl: empty symbols, bottom curves) and different total aluminum concentrations. (diamonds: $14.3 \pm 2.2 \mu\text{M}$; triangles: $34.8 \pm 5.7 \mu\text{M}$; squares: $108.1 \pm 4.4 \mu\text{M}$; see Table 1 for the exact concentration in each experiment). All lines were computed with a single model which takes into account both cation exchange and surface complexation on edges. The different lines correspond to the different experimental conditions (Experiments 10 to 21, Table 1).

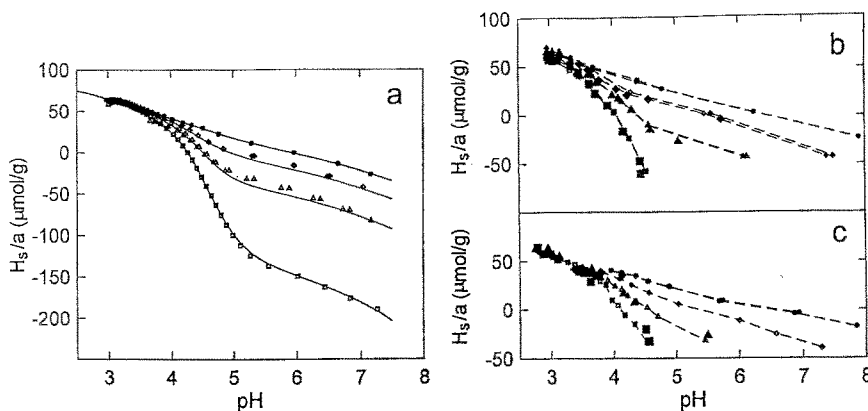


Figure 4. Proton surface charge on montmorillonite as a function of aluminum adsorption (see text for definitions) in $\mu\text{mol/g}$ vs. pH, at three different KCl background ionic strengths (1 M, Figure 4a; 0.1 M, Figure 4b; 0.03 M, Figure 4c) and at four different total added aluminum concentrations (in each plot: upper curves: 0 M; upper middle curve: $14.32 \pm 2.23 \mu\text{M}$; lower middle curve: $34.8 \pm 5.7 \mu\text{M}$; lower curve: $108.1 \pm 4.4 \mu\text{M}$; see Table 1 for individual values). The lines in Figure 4a are modeled curves.

$pqr = 1, 1, -1$, $1, 1, -2$ and $1, 1, -3$, i.e. by assuming three simultaneous adsorption mechanisms with $\log \beta_{pqr}^s$ values of 1.57, -4.35 , -11.37 , respectively (Fig. 3 and 4a). Acid base properties of montmorillonite (see upper curve in Fig. 4a) are described by Equation (2) with $pqr = 1, 0, 1$ and $1, 1, -1$ and $\log \beta_{pqr}^s$ values of 4.80 and -6.96 , respectively, assuming an electrical double layer with a specific capacitance constant of 5.5 F m^{-2} , a surface area of $15 \text{ m}^2 \text{ g}^{-1}$, the edges accounting for about 2% of the $750 \text{ m}^2 \text{ g}^{-1}$ total specific surface area (Sposito, 1984), and a site density of $86.4 \mu\text{mol g}^{-1}$. The resulting site density of $3.46 \text{ sites nm}^{-2}$ is in good agreement with values derived from crystal growth theory (White and Zelazny, 1988).

Aluminum adsorption data obtained at the two low ionic strengths (0.1 M and 0.03 M) are above pH 3.5 of the same nature to those obtained in the 1 M ionic strength medium, with a shift of the steep part of the adsorption curve to lower pH as the ionic strength is decreased (Fig. 3). However at lower pH values ($3 < \text{pH} < 3.5$), the amount of aluminum adsorbed is nearly constant and dependent of pH (20% adsorption for 0.1 M K^+ , and around 90% adsorption with 0.03 M K^+). This adsorption obviously involves another mechanism.

Insights into the adsorption mechanisms of aluminum above and below pH 3.5 are provided by the proton titration curves (Fig. 4). The proton titration curve of the (Al, K)-montmorillonite coincides with that of K-montmorillonite up to about pH 3.5 and is independent of the ionic strength and thus of the amount of aluminum adsorbed. Above this value, the titration curves diverge. Therefore two types of mechanism are recognized for the adsorption of aluminum ions on montmorillonite. A first mechanism in which the adsorption of aluminum and its hydrolysis are linked together, as described by the Equation (2), and another one responsible for the adsorption observed at low pH and

low K^+ concentrations ($[K^+] \leq 0.1$ M) in which no proton release is observed as Al^{3+} is adsorbed. This second mechanism is a K^+/Al^{3+} cation exchange, which can be described (Fig. 3 and 4) in the classical thermodynamic treatment by the Vanselow coefficient K_v , with: $\log K_v = -0.75 \pm 0.05$. No correction for the surface activity coefficient could be performed, due to the limited range of adsorbed Al equivalent fraction explored in this study. The value of the K^+/Al^{3+} exchange coefficient K_v , is in good agreement with values reported in the literature for K_n ($-1.57 < \log K_n < 0.612$; Bruggenwert and Kamphorst, 1979). K_n is an exchange coefficient computed on the basis of equivalent fraction instead of mole fraction for the surface species, and at low Al surface coverage $K_v \approx K_n$.

Discussion

In concentrated salt solution (1 M KCl) montmorillonite behavior with respect to Al adsorption (Fig. 3) and proton desorption (Fig. 4), is comparable to that on oxides such as silica, goethite and lepidocrocite (Fig. 2). Thus at high ionic strengths Al species cannot compete with K^+ for adsorption on basal planes. Adherence of data to the model suggest that Al species adsorb on $\equiv SOH$ amphoteric surface hydroxyl sites. The acid-base properties of this site appear to vary considerably depending on the mineral pre-treatment. Point of zero net proton charge (PZNPC which is equal to $(\log \beta_{1,0,-1(int)} - \log \beta_{1,0,1(int)})/2$) reported in the literature range from 5.88 (this work; with K-saturated montmorillonite titrated starting at pH 3 after a short equilibration time), 8.0 (Zysset, 1992; for the same K-saturated montmorillonite, but starting the titration at PZNPC), 8.44 (Stadler and Schindler, 1993; for a Ca-montmorillonite titrated starting at pH 3.5 after a week equilibration time), and 10.54 (Goldberg and Glaubig, 1986; for an untreated montmorillonite). The $\equiv SOH$ component symbolizes a moiety present on the crystal edges of montmorillonite and which may include, according to crystal field theory, Si(IV) tetrahedra single corners (singly coordinated silanol groups) and protruding Al(III) octahedra edges, i.e. pairs of singly coordinated aluminol groups (White and Zelazny, 1988). The oxygen atoms shared by Si(IV) tetrahedra and non-protruding Al(III) octahedra are very weak Lewis acids and can be considered as non-reactive. Given the above mentioned scatter in $\equiv SOH$ acid-base properties, no attempt will be made to identify the microscopic structural group present on the edges and responsible for the macroscopic acid-base behavior.

Amphoteric properties of the $\equiv SOH$ site are furthermore at variance with properties of hydroxyl groups present at the surface of oxides, in the sense that their proton charge is almost independent of ionic strength (compare top curves in Fig. 4a, 4b, and 4c). This property leads to a very large value of the specific surface capacitance (5.5 F m^{-2}), suggesting that protonated and deprotonated sites are not present as free $\equiv SOH_2^+$ or $\equiv SO^-$ species (neutralized by charges present in the diffuse ion swarm) but rather as neutral $\equiv SOH_2^+ Cl^-$ and $\equiv SO^- K^+$ species, and this, whatever the ionic strength. This observation is in agreement with recent electroacoustic measurements performed on kaolinite indicating that most of the surface charge (rising from edge site protonation/deprotonation) is balanced by

monovalent ions which are so strongly adsorbed that these complexes contribute nothing to the electrokinetic charge, even in a 10^{-3} M background ionic medium (Hunter and James, 1992).

A second sorption mechanism is favored at pH values below 3.75. This mechanism is (i) pH independent, (ii) highly dependent on ionic strength and (iii) does not involve proton exchange (Fig. 4). This adsorption is attributed to K^+/Al^{3+} cation exchange occurring on the basal plane of montmorillonite. The two mechanisms, namely (1) complexation with surface hydroxyl groups and (2) cation exchange on the negatively charged basal plane, may account for the various effects of sorbed Al(III) on montmorillonite dissolution. At pH 3.0, sorbed Al(III) in 0.1 M ionic medium has no effect on montmorillonite dissolution, whereas it inhibits this dissolution at pH 4.0 (Zysset, 1992). This may be interpreted as follows. At pH 4.0, aluminum ions are sorbed on the crystal broken edge (the active crystal growth plane) as an inner-sphere complex. In this complex aluminum octahedra presumably shares edges (defined here as a pair of neighbor oxygen atoms in the octahedra) with structural Al octahedra, and single corners with Si tetrahedra. Therefore it reduces the number of low coordination Si tetrahedra, and inhibits their detachment, and thus the dissolution of montmorillonite. This effect is similar to that observed on pure silica (Iler, 1973). On the contrary, aluminum ions sorbed at low pH values are expected to be present on the montmorillonite basal plane, as hydrated Al(III) ions. These ions, which are fully exchangeable by K^+ ions have no more effect than K^+ ions on the weathering of montmorillonite.

The observations reported in this study and in Zysset's work (1992) suggest therefore the presence of two different sites for Al(III) binding.

1. A weakly acidic $\equiv XH$ group that account for ion exchange and aluminum adsorption below pH 3.3. The surface functional group is the siloxane ditrigonal cavity present on the basal plane of montmorillonite and has the properties of a weakly acid group (Sposito, 1984; Schindler et al., 1987). Under the chosen experimental conditions, the functional group seems to be fully deprotonated, since the surface proton charge, and thus the functional group dissociation, is independent of the Al^{3+} sorbed mole fraction (Fig. 4).

2. An amphoteric surface hydroxyl $\equiv SOH$ group which can bind and release protons (to form $\equiv SOH_2^+ Cl^-$ and $\equiv SOH^- K^+$) and accounts for the adsorption of aluminum at higher pH values. The hydroxyl sites differ from those on oxides as they develop very small surface potential on their own (as indicated by the very large value for the surface capacitance). This phenomenon is probably due to the overwhelmingly large and constant potential developed on the faces of montmorillonite in response to the structural charge.

Adsorption of trace metal ions is therefore dominated by two different mechanisms, depending on pH. This conclusion is valid not only for Al^{3+} , but also for Cu^{2+} , Zn^{2+} (Fig. 2), Pb^{2+} (Wold and Pickering, 1981) and UO_2^{2+} (Payne and Waite, 1991). In all these studies, the trace element is present at a total concentration lower than the concentration of montmorillonite crystal edge sites. At low pH values the amount of sorbed metal ion at a given ionic strength is nearly constant. This is the field of true cation exchange. At higher pH values, a step increase of adsorption is observed. Comparison of top and bottom curves in Figure 2 indicates that this critical pH value is nearly identical for silica and for montmorillonite.

Conclusion

Adsorption of trace metal ions on montmorillonite appears to be due to:

1. True cation exchange at the permanently charged surface sites, up to the pH at which the metal starts to significantly adsorb on pure silica at comparable metal to surface site ratio. The amount of trace element sorbed by cation exchange is highly dependent on the ionic strength of the background ionic medium, according to mass action laws (Equation (13)).

2. Surface complexation involving the particle edge surfaces, at higher pH values. The amount sorbed on these surfaces changes drastically, as it does on oxides, with small pH increase.

Since an abundant literature already exists on the pH-dependence of metal ion adsorption on oxides, the above rough rule of thumb indicating the pH at which trace metal ion adsorption shifts from cation exchange to surface complexation may help to predict the retardation imposed by bentonite geochemical barriers, given the ambient pH, on the transport of a given exotic element. This is most important as bentonite is a candidate backfill material for repositories of spent nuclear fuel and is extensively used as barrier material for hazardous waste dumping sites.

ACKNOWLEDGMENTS

At this point we all would like to thank Paul for the wonderful atmosphere he created in his laboratory at the University of Bern. This work was financially supported by the Swiss National Science Foundation (Project 2-5636). L. C. thanks Dr. Steven Short and Dr. A. Manceau for valuable discussion, and B. Trusch for technical assistance. Helpful reviews were provided by E. Silvester and C. Eggleston.

REFERENCES

- Biederman, G., J. Bruno, D. Ferri, I. Grenthe, F. Salvatore and K. Spathiu, 1982. *Mat. Res. Soc. Symp. Ser.* 11:791.
- Brown, C. S. and L. A. Thomas, 1960. The effect of impurities on the growth of synthetic quartz. *J. Phys. Chem. Solids* 13:337–342.
- Bruggenwert, M. G. M. and A. Kamphorst, 1979. Survey of experimental information on cation exchange in soil systems. In: G. H. Bolt (ed.) *Soil Chemistry B. Physicochemical Models*. Elsevier, Amsterdam. pp. 141–203.
- Charlet, L. and A. Manceau, 1993. Structure, formation and reactivity of hydrous oxide particles: In: J. Buffle and H. P. van Leeuwen (eds.), *Environmental Particles II*. Lewis Publ., pp. 117–164.
- Dent, A. J., J. D. F. Ramsay and S. W. Swanton, 1992. An EXAFS study of uranyl ion in solution and sorbed onto silica and montmorillonite clay colloids. *J. Colloid Interface Sci.* 150:45–60.
- Dougan, W. K. and A. L. Wilson, 1974. The absorptiometric determination of aluminum in water. A comparison of some chromogenic reagents and the development of an improved method. *Analyst* 99:413–430.
- Fletcher, P. and G. Sposito, 1989. The chemical modelling of clay/electrolyte interactions for montmorillonite. *Clay Minerals* 24:375–391.
- Goldberg, S. and R. A. Glaubig, 1986. Boron adsorption and silicon release by the clay minerals kaolinite, montmorillonite and illite. *Soil Sci. Soc. Am. J.* 50:1442–1448.

- Hedlund, T., 1988. Studies of complexation and precipitation equilibria in some aqueous aluminum(III) systems. Ph.D. Thesis. Umeå University, Umeå, Sweden.
- Hunter, R.J. and M. James, 1992. Charge reversal of kaolinite by hydrolyzable metal ions: an electroacoustic study. *Clays Clay Minerals* 40:644–649.
- Iler, R. K., 1973. Effect of adsorbed alumina on the solubility of amorphous silica in water. *J. Colloid Interface Sci.* 43:399–408.
- Lövgren, L., S. Sjöberg, and P. W. Schindler, 1990. Acid/base reactions and Al(III) complexation at the surface of goethite. *Geochim. Cosmochim. Acta* 54:1301–1306.
- McBride, M. B., 1991. Processes of heavy and transition metal sorption by soil minerals. In: G. H. Bolt, F. DeBoot, M. H. B. Hayes and M. D. McBride (ed.) *Interactions at the Soil Colloid-Soil Solution Interface*. Kluwer Academic Press, The Netherlands. p. 149–175.
- Motschi, H., 1987. Aspects of the molecular structure in surface complexes: Spectroscopic investigations. In: W. Stumm (ed.) *Aquatic Surface Chemistry*. John Wiley & Sons. p. 111–126.
- Payne, T. E. and T. D. Waite, 1991. Surface complexation modelling of uranium sorption data obtained by isotopic exchange techniques. *Radiochim. Acta* 52/53:487–493.
- Schindler, P. W., B. Fürst, R. Dick and P. U. Wolf, 1976. Ligand properties of surface silanol groups: I. Surface complex formation with Fe^{2+} , Cu^{2+} , Cd^{2+} and Pb^{2+} . *J. Colloid Interface Sci.* 55: 469–475.
- Schindler, P. W. and W. Stumm, 1987. The surface chemistry of oxides, hydroxides and oxide minerals. In: W. Stumm (ed.), *Aquatic Surface Chemistry*. John Wiley & Sons. p. 83–110.
- Schindler, P. W., P. Lietchi, and J. C. Westall., 1987. Adsorption of copper, cadmium and lead from aqueous solution to the kaolinite/water interface. *Netherlands J. Agri. Sci.* 35:219–230.
- Shaviv, A. and S. V. Mattigod, 1985. Cation exchange equilibria in soils expressed as cation-ligand complex formation. *Soil Sci Soc. Am. J.* 49:569–573.
- Sposito, G., 1984. *Surface Chemistry of Soils*. Oxford University press, Oxford. 223 pp.
- Sposito, G., K. M. Holtzclaw, C. T. Johnston and C. S. Le Vesque-Madore, 1981. Thermodynamics of sodium-copper exchange on Wyoming bentonite at 298 K. *Soil Sci. Soc. Am. J.* 45:1079–1084.
- Stadler, M. and P. W. Schindler, 1993. Modeling of H^+ and Cu^{2+} adsorption on calcium montmorillonite. *Clays Clay Minerals* 41:288–296.
- Westall, J. C., 1982. FITEQL. A computer program for determination of chemical equilibrium constants from experimental data. Version 1.2, Report 82-01, Oregon State University, Corvallis, Oregon.
- Wold, J. and W. F. Pickering, 1981. Influence of electrolytes on metal ion sorption by clays. *Chem. Geol.*, 33:91–99.
- Wolery, P. J., 1992. EQ 3/6: A software package for geochemical modeling of aqueous systems: package overview and installation guide. UCRL/MA/10662/Part I.
- White, G. N. and L. W. Zelazny, 1988. Analysis and implications of the edge structure of dioctahedral phyllosilicates. *Clays Clay Minerals* 36:141–146.
- Zhang, Y., L. Charlet and P. W. Schindler, 1992. Adsorption of protons, Fe(II) and Al(III) on lepidocrocite ($\gamma\text{-FeOOH}$). *Colloids Surf.* 62:259–268.
- Zysset, M., 1992. Die protoneninduzierte Auflösung von K-Montmorillonit. Ph.D. Thesis. Bern University, Bern, Switzerland.